

# Table Cartograms

William Evans<sup>1</sup>, Stefan Felsner<sup>2</sup>, Michael Kaufmann<sup>3</sup>, Stephen G. Kobourov<sup>4</sup>,  
Debajyoti Mondal<sup>5</sup>, Rahnuma Islam Nishat<sup>6</sup>, and Kevin Verbeek<sup>7</sup>

<sup>1</sup>Department of Computer Science, University of British Columbia

<sup>2</sup>Institut für Mathematik, Technische Universität Berlin

<sup>3</sup>Wilhelm-Schickard-Institut für Informatik, Universität Tübingen

<sup>4</sup>Department of Computer Science, University of Arizona

<sup>5</sup>Department of Computer Science, University of Manitoba

<sup>6</sup>Department of Computer Science, University of Victoria

<sup>7</sup>Department of Computer Science, University of California, Santa Barbara

**Abstract.** A table cartogram of a two dimensional  $m \times n$  table  $A$  of non-negative weights in a rectangle  $R$ , whose area equals the sum of the weights, is a partition of  $R$  into convex quadrilateral faces corresponding to the cells of  $A$  such that each face has the same adjacency as its corresponding cell and has area equal to the cell's weight. Such a partition acts as a natural way to visualize table data arising in various fields of research. In this paper, we give a  $O(mn)$ -time algorithm to find a table cartogram in a rectangle. We then generalize our algorithm to obtain table cartograms inside arbitrary convex quadrangles, circles, and finally, on the surface of cylinders and spheres.

## 1 Introduction

A *cartogram*, or *value-by-area diagram*, is a thematic cartographic visualization, in which the areas of countries are modified in order to represent a given set of values, such as population, gross-domestic product, or other geo-referenced statistical data. Red-and-blue population cartograms of the United States were often used to illustrate the results in the 2000 and 2004 presidential elections. While geographically accurate maps seemed to show an overwhelming victory for George W. Bush, population cartograms effectively communicated the near 50-50 split, by deflating the rural and suburban central states.

The challenge in creating a good cartogram is thus to shrink or grow the regions in a map so that they faithfully reflect the set of pre-specified area values, while still retaining their characteristic shapes, relative positions, and adjacencies as much as possible. In this paper we introduce a new *table cartogram* model, where the input is a two dimensional  $m \times n$  table of non-negative weights, and the output is a rectangle with area equal to the sum of the input weights partitioned into  $m \times n$  convex quadrilateral faces each with area equal to the corresponding input weight. Fig. 1 shows two such examples. Such a visualization preserves both area and adjacencies, furthermore, it is simple, visually attractive, and applicable to many fields that require visualization of data table.

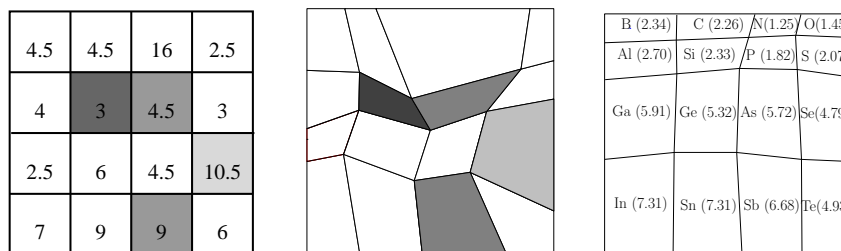


**Fig. 1.** A  $4 \times 4$  table, its table cartogram, and a cartogram of some elements of the periodic table according to their density in grams per cubic centimeter (for solids) or per liter (for gases).

The solution to the problem is not obvious even for a  $2 \times 2$  table. For example, Fig. 2(a–b) shows a table  $A$  and a unit square  $R$ . One attempt to find the cartogram of  $A$  in  $R$  may be to first split  $R$  horizontally according to the sum of each row, and then to find a good split in each subrectangle to realize the correct areas. But this approach does not work, because the first split prevents the creation of the two convex quadrilaterals with area  $\epsilon$  in opposite corners that share a boundary vertex, Fig. 2(c). Fig. 2(d) shows a possible cartogram.

The following little argument shows that  $2 \times 2$  table cartograms exist. The argument contains some elements that will be reused for the general case. The input is a  $2 \times 2$  table with four positive reals  $a, b, c, d$  with  $a + b + c + d = 1$ , as shown in Fig. 2(e). Rotational symmetry of the problem allows us to assume that  $a + b \leq 1/2$ . Fix the unit square  $R$  with corners  $(0, 0), (0, 1), (1, 1), (1, 0)$  as the frame for the table cartogram. Now consider the horizontal line  $\ell$  with the property that every triangle  $T(p)$  with top side equal to the top side of  $R$  and one corner  $p$  on  $\ell$  has area  $a + b$ . Since  $a + b \leq 1/2$ , the line  $\ell$  intersects  $R$  in a horizontal segment. For  $p \in \ell \cap R$ , the vertical line through  $p$  partitions  $R \setminus T(p)$  into a left 4-gon  $S^-$  and a right 4-gon  $S^+$ . The areas of these two 4-gons depend continuously on the position of point  $p$  but their sum is always  $c + d$ . If  $p$  is on the left boundary,  $Area(S^+) = c + d$ , and if  $p$  is on the right boundary,  $Area(S^+) = 0$ . Hence, it follows from the intermediate value theorem that there is a position for  $p$  on  $\ell \cap R$  such that  $Area(S^-) = c$  and  $Area(S^+) = d$ . By rotating a line around this  $p$ , we find a line that partitions  $T(p)$  such that the

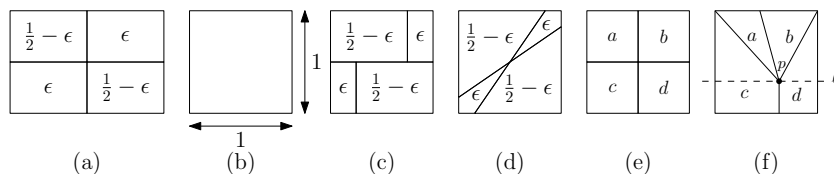


**Fig. 2.** (a) A  $2 \times 2$  table  $A$ . (b)  $R$ . (c) An attempt to find a cartogram. (d) A cartogram of  $A$  in  $R$ . (e) A  $2 \times 2$  table  $A$ . (f) The cartogram showing  $\ell$  as a dashed line.

left triangle has area  $a$  and thus the right triangle has area  $b$ , this again uses the intermediate value theorem. The resulting partition of  $R$  into four parts is a table cartogram for the input table, see Fig. 2(f). The critical reader may object that two of the 4-gons have a degenerate side. This can be avoided by perturbing the cartogram slightly to make a very short edge instead of a point. The result is an  $\varepsilon$  approximate cartogram without degeneracies. Another approach is to modify the construction rules so that degeneracies are avoided. We take this approach in Section 2 to show the existence of non-degenerate table cartograms in general.

**Related Work.** The problem of representing additional information on top of a geographic map dates back to the 19th century, and highly schematized rectangular cartograms can be found in the 1934 work of Raisz [16]. Recently, van Kreveld and Speckmann describe automated methods to produce rectangular cartograms [19]. With such rectangular cartograms it is not always possible to represent all adjacencies and areas accurately [12, 19]. However, in many “simple” cases, such as France, Italy and the USA, rectangular cartograms and even table cartograms offer a practical and straightforward schematization, e.g., Fig. 3. *Grid maps* are a special case of single-level spatial treemaps: the input is a geographic map mapped onto a grid of equal-sized rectangles, in such a way as to preserve as well as possible the relative positions of the corresponding regions [20, 9]. As we show, such maps can always be visualized as table cartograms.

Eppstein *et al.* studied area-universal rectangular layouts and characterized the class of rectangular layouts for which all area-assignments can be achieved with combinatorially equivalent layouts [8]. If the requirement that rectangles are used is relaxed to allow the use of rectilinear regions then de Berg *et al.* [4] showed that all adjacencies can be preserved and all areas can be realized with 40-sided regions. In a series of papers the polygon complexity that is sufficient to realize any rectilinear cartogram was decreased from 40 sides down to 8 sides [2], which is best possible due to an earlier lower bound [21].

More general cartograms without restrictions to rectangular or rectilinear shapes have also been studied. For example adjacencies can be preserved and

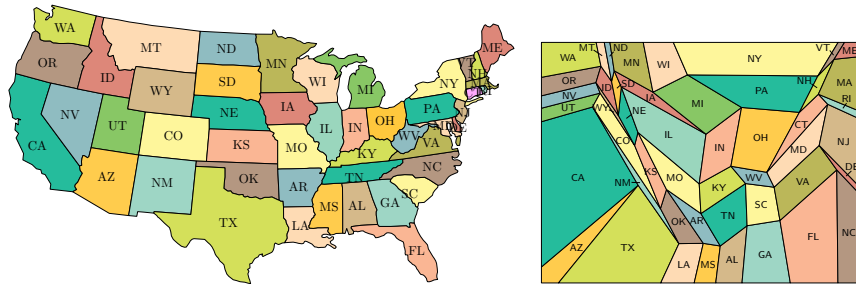


**Fig. 3.** A table cartogram of USA according to the population of the states in 2010, using the grid map of [9]. See Fig. 9 for the data table.

areas represented perfectly using convex quadrilaterals if the dual of the map is an outerplanar graph [1]. Dougenik *et al.* introduced a method based on force fields where the map is divided into cells and every cell has a force related to its data value which affects the other cells [6]. Dorling used a cellular automaton approach, where regions exchange cells until an equilibrium has been achieved, i.e., each region has attained the desired number of cells [5]. This technique can result in significant distortions, thereby reducing readability and recognizability. Keim *et al.* defined a distance between the original map and the cartogram with a metric based on Fourier transforms, and then used a scan-line algorithm to reposition the edges so as to optimize the metric [14]. Gastner and Newman [11] project the original map onto a distorted grid, calculated so that cell areas match the pre-defined values. The desired areas are then achieved via an iterative diffusion process inspired by physical intuition. The cartograms produced this way are mostly readable but the complexity of the polygons can increase significantly. Edelsbrunner and Waupotitsch [7] generated cartograms using a sequence of homeomorphic deformations. Kocmoud and House [13] described a technique that combines the cell-based approach of Dorling [5] with the homeomorphic deformations of Edelsbrunner and Waupotitsch [7].

There are thousands of papers, spanning over a century, and covering various aspects of cartograms, from geography to geometry and from interactive visualization to graph theory and topology. The above brief review is woefully incomplete; the survey by Tobler [18] provides a more comprehensive overview.

**Our Results.** The main construction is presented in Section 2. We start with a simple constructive algorithm that realizes any table inside a rectangle in which each cell is represented by a convex quadrilateral with its prescribed weight. The approach relies on making many of the regions be triangles. We then modify the method to remove such degeneracies. The construction can be implemented to run in  $O(mn)$  time, i.e., in time linear in the input size.

In Section 3 we find table cartograms inside arbitrary triangles or convex quadrilaterals, which is best possible, because regular  $n$ -gons,  $n \geq 5$ , do not always support table cartograms (e.g., consider a table with some cell value larger than the maximum-area convex quadrangle that can be drawn inside the  $n$ -gon). We also realize table cartograms inside circles, using circular-arcs, and on the surface of a sphere via a transformation from a realization on the cylinder.

## 2 Table cartograms in rectangles

We first construct a cartogram with degenerate 4-gons. The input is a table  $A$  with  $m$  rows and  $n$  columns of non-negative numbers  $A_{i,j}$ . Let  $S = \sum_{i,j} A_{i,j}$  and let  $S_i$  be the sum of the numbers in row  $i$ , i.e.,  $S_i = \sum_{1 \leq j \leq n} A_{i,j}$ . Assume, by scaling, that  $S > 4$ . Let  $R$  be the rectangle with corners  $(0, 0)$ ,  $(S/2, 0)$ ,  $(S/2, 2)$ ,  $(0, 2)$ . We construct the cartogram within  $R$  and later generalize the construction to all rectangles with area  $S$ . Let  $k$  be the largest index such that the sum of the numbers in rows  $1, 2, \dots, k - 1$  is less than  $S/2$ . We may then

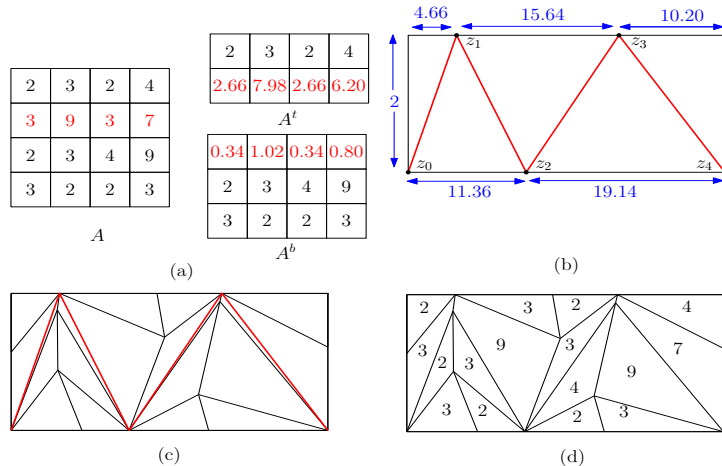


**Fig. 4.** (a) Illustration for  $A$ ,  $A^t$  and  $A^b$ , where  $k = 2$  and  $\lambda \approx 0.886$ . (b) The zigzag path  $Z$ . We have distorted the aspect ratio of the figure to increase readability. (c) The subdivision of triangles, where  $Z$  is shown in red, and (d) the complete cartogram.

choose  $\lambda \in (0, 1]$  such that  $\sum_{1 \leq i \leq k-1} S_i + \lambda S_k = S/2$ . We split the table  $A$  into two tables  $A^t$  and  $A^b$ . Table  $A^t$  consists of  $k$  rows and  $n$  columns. The first  $k-1$  rows are taken from  $A$ , i.e.,  $A^t_{i,j} = A_{i,j}$  for  $1 \leq i \leq k-1$  and  $1 \leq j \leq n$ . The last row is a  $\lambda$ -fraction of row  $k$  from  $A$ , i.e.,  $A^t_{k,j} = \lambda \cdot A_{k,j}$  for all  $j$ . Table  $A^b$  consists of  $m-k+1$  rows and  $n$  columns. The first row accommodates the remaining portion of row  $k$  from  $A$ , i.e.,  $A^b_{1,j} = (1-\lambda) \cdot A_{k,j}$ . All the other rows are taken from  $A$ , i.e.,  $A^b_{i,j} = A_{i+k-1,j}$  for  $i > 1$  and all  $j$ . An example is shown in Fig. 4(a). If  $\lambda = 1$ , then  $A^b$  contains a top row of zeros.

Let  $D_j^t$  be the sum of entries in columns  $2j-2$  and  $2j-1$  from  $A^t$ , where  $1 \leq j \leq \lfloor m/2 + 1 \rfloor$ . Note that  $D_1^t$  is only responsible for one column. The same may hold for the last  $D_j^t$  depending on the parity of  $m$ . Similarly,  $D_l^b$  is the sum of entries in columns  $2l-1$  and  $2l$  from  $A^b$ , where  $1 \leq l \leq \lceil m/2 \rceil$ . Again, depending on the parity of  $m$  the last  $D_l^b$  may only be responsible for one column.

We now define a zig-zag  $Z$  in  $R$  (formally,  $Z$  is a polygonal line) such that the areas of the triangles defined by  $Z$  are the numbers  $D_1^t, D_1^b, D_2^t, D_2^b, D_3^t, \dots$  in this order. The zig-zag starts at  $z_0 = (0, 0)$ . Since the height of  $R$  is 2, the first segment ends at  $z_1 = (D_1^t, 2)$  and the second segment goes down to  $z_2 = (D_1^b, 0)$ . In general, for  $i$  odd,  $z_i = (\sum_{j=1}^{\lceil i/2 \rceil} D_j^t, 2)$  and for  $i$  even,  $z_i = (\sum_{l=1}^{i/2} D_l^b, 0)$ . An important property of  $Z$  is that it ends at one of the two corners on the right side of  $R$ . This is because  $\sum_j D_j^t = S/2 = \sum_l D_l^b$ .

Lemma 2 shows that we can partition each triangle created by the zig-zag  $Z$  into triangles whose areas are the corresponding entries in  $A^t$  or  $A^b$ . It relies on the following lemma which is a consequence of properties of barycentric coordinates. The proof is in Appendix A.

**Lemma 1 (Triangle Lemma).** *Let  $\triangle abc$  be a triangle and let  $\alpha, \beta, \gamma$  be non-negative numbers, where  $\alpha + \beta + \gamma = \text{Area}(\triangle abc)$ . Then we can find a point  $p$  in  $\triangle abc$ , where  $\text{Area}(\triangle pbc) = \alpha$ ,  $\text{Area}(\triangle apc) = \beta$ ,  $\text{Area}(\triangle abp) = \gamma$ , in  $O(1)$  arithmetic operations.*

**Lemma 2.** *Let  $A$  be a  $m \times 2$  table such that each cell is assigned a non-negative number. Let  $\triangle abc$  be a triangle such that the area of  $\triangle abc$  is equal to the sum of the numbers of  $A$ . Then  $A$  admits a cartogram inside  $\triangle abc$  such that all cells of  $A$  are represented by triangles and the boundary between those triangles representing cells in the left column and those representing cells in the right column is a polygonal path connecting point  $a$  to some point on the segment  $bc$ .*

*Proof.* The proof is by induction on  $m$ . The case  $m = 1$  is obvious. If  $m > 1$  we define  $\alpha = \sum_{1 \leq i \leq m-1} A_{i,1} + A_{i,2}$ ,  $\beta = A_{m,1}$  and  $\gamma = A_{m,2}$ . Using Lemma 1 we find a point  $p$  in  $\triangle abc$  that partitions the triangle into triangles of areas  $\alpha$ ,  $\beta$  and  $\gamma$ . We keep the triangles  $\triangle apc$  and  $\triangle abp$  as representatives for  $A_{m,1}$  and  $A_{m,2}$  and construct the cartogram for the first  $m - 1$  rows of  $A$  in the triangle  $\triangle pbc$  by induction.  $\square$

To partition triangle  $\triangle z_{2j-2}, z_{2j-3}, z_{2j-1}$ , for  $1 \leq j \leq \lfloor m/2 + 1 \rfloor$  (where  $z_{-1} = (0, 2)$  and  $z_{m+1} = (S/2, 2)$  if needed), we appeal to Lemma 2 with  $A$  (in the lemma) being the two columns from  $A^t$  whose sum is  $D_j^t$ . To make Lemma 2 applicable to cases like  $D_1^t$  which represent only one column from  $A^t$ , we simply add a column of zeros to  $A$ . Similarly, we can partition triangle  $\triangle z_{2l-1}, z_{2l-2}, z_{2l}$ , for  $1 \leq l \leq \lceil m/2 \rceil$ .

This yields a table cartogram of the  $(m+1) \times n$  table  $A^+$  that is obtained by stacking  $A^t$  on  $A^b$ . Note, however, that all triangles representing cells from the last row of  $A^t$  have a side that equals one of the edges of  $Z$ . Symmetrically, all triangles representing cells from the first row of  $A^b$  have a side on  $Z$ . Hence, by removing the edge of  $Z$  we glue two triangles of area  $\lambda A_{k,j}$  and  $(1 - \lambda)A_{k,j}$  into a 4-gon of area  $A_{k,j}$ . The 4-gons obtained by removing edges of  $Z$  are convex because they have crossing diagonals. This completes the construction.

To complete the proof of the following theorem, in which  $R$  is a  $w \times h$  rectangle with area  $S$ , we scale the above cartogram by a factor of  $h/2$  vertically and a factor of  $2/h$  horizontally.

**Theorem 1.** *Let  $A$  be a  $m \times n$  table of non-negative numbers  $A_{i,j}$ . Let  $R$  be a rectangle with width  $w$ , height  $h$  and area equal to the sum of the numbers of  $A$ . Then there exists a cartogram of  $A$  in  $R$  such that every face in the cartogram is convex. The construction requires  $O(mn)$  arithmetic operations.*

**Removing degeneracies.** The construction of the proof of Theorem 1 creates faces of degenerate shape, i.e., some faces may not be perfect quadrangles. We modify this construction to avoid the degeneracies. Of course we have to make a stronger assumption on the input: All entries  $A_{i,j}$  of the table are strictly positive. The first part of the construction remains unaltered.

- Determine  $k$  and  $\lambda$  such that  $\sum_{1 \leq i \leq k-1} S_i + \lambda S_k = S/2$ .

- Define  $A^t$  and  $A^b$  and the two-column sums  $D_j^t$  and  $D_l^b$  for these tables.
- Compute the zig-zag in the rectangle  $R$  of height 2 and width  $S/2$ .

Let  $z_0, z_1, \dots, z_n$  be the corner points of the zig-zag  $Z$ . For  $i$  even we define  $z'_i = z_i + (0, v)$  and for  $i$  odd  $z'_i = z_i - (0, v)$ , i.e.,  $z'_i$  is obtained by shifting  $z_i$  vertically a distance of  $v$  into  $R$ . We will choose this positive value  $v$  to obey conditions (B1) and (B2) required by the construction. Let  $Z'$  be the zig-zag with corners  $z'_0, z'_1, \dots, z'_n$ . The segment  $z'_i, z_i$  is the *leg at  $z'_i$* . The union of all the legs and  $Z'$  is the *skeleton  $G'$*  of a partition of  $R$  into 5-gons. We refer to the 5-gons with corners  $z_{i-1}, z_{i+1}, z'_{i+1}, z'_i, z'_{i-1}$  as  $F_i$ . We abstain from introducing extra notation for the two 4-gons at the ends of  $Z'$  and just think of them as degenerate 5-gons.

**Lemma 3.** *A 5-gon in  $R$  with vertices  $(x_1, 0), (x_3, 0), (x_3, v), (x_2, 2 - v), (x_1, v)$  has the same area  $x_3 - x_1$  as the triangle with corners  $(x_1, 0), (x_3, 0), (x_2, 2)$ .*

*Proof.* First note that changing the value of  $x_2$  (shear) preserves the area of the 5-gon and of the triangle. Hence we may assume that  $x_2 = x_3$ . Now let  $P$  be the parallelogram with corners  $(x_1, 0), (x_1, v), (x_2, 2), (x_2, 2 - v)$ . Both, the 5-gon and the triangle can be partitioned into the triangle  $(x_1, 0), (x_2, 2 - v), (x_3, 0)$  and a triangle that makes a half of  $P$ .  $\square$

Some of the 5-gons  $F_i$  may not be convex. However, concave corners can only be at  $z'_{i+1}$  or  $z'_{i-1}$ . To get rid of concave corners we deal with corners at  $z'_1, z'_2, \dots, z'_{n-1}$  in this order. At each  $z'_i$  we may slightly shift  $z'_i$  horizontally and bend the leg to rebalance the areas. This can be done so that the concave corner at  $z'_i$  is resolved. We then say that  $z'_i$  has been *convexified*. Fig. 5 shows an example of the process.

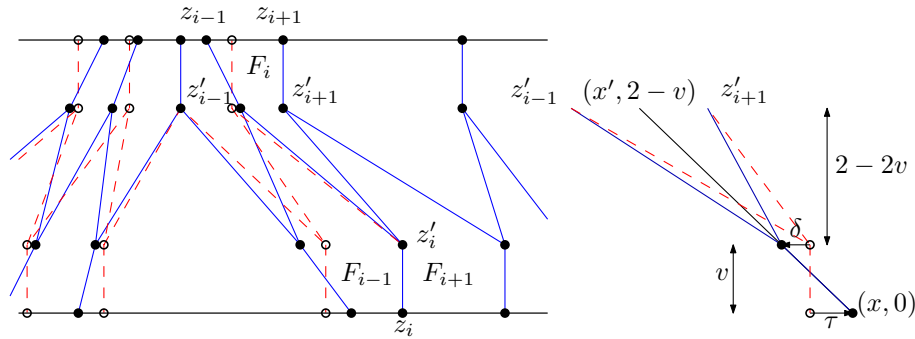


**Fig. 5.** Before and after convexifying  $z'_i$ . The dashed lines represent the original  $Z'$ .

The vertex  $z'_i$  has a concave corner in at most one of  $F_{i-1}$  and  $F_{i+1}$ . In the first case we move  $z'_i$  to the right in the second case we move  $z'_i$  to the left. By symmetry, we only detail the second case, i.e.,  $z'_i$  has a concave corner in  $F_{i+1}$ .

Shifting  $z'_i$  horizontally keeps the area of  $F_i$  invariant, only the areas of  $F_{i-1}$  and  $F_{i+1}$  are affected by the shift. By shifting  $z'_i$  a distance of  $\delta$  to the left while

keeping  $z_i$  at its place the increase in area of  $F_{i+1}$  is  $\delta(2-v)/2$ . To balance the increase we move  $z_i$ , the other end of the leg, to the right by an amount  $\tau$ , where  $\tau v/2 = \delta(2-v)/2$ . To make sure that the corners at  $z'_i$  after shifting are convex we choose  $\delta$  and  $\tau$  so that the line connecting the new positions of  $z_i$  and  $z'_i$  contains the midpoint of  $z'_{i-1}$  and  $z'_{i+1}$ . If the new position of  $z_i$  is  $(x, 0)$  and  $(x', 2-v)$  is the midpoint of  $z'_{i-1}$  and  $z'_{i+1}$  then  $v/(\tau + \delta) = 2/(x - x')$ .

We do not want the shift of  $z_i$  to introduce a crossing. We ensure this with a bound on  $v$ . For all  $j$ , let  $T_j = \text{Area}(F_j)$  and recall that this is the distance between  $z_{j-1}$  and  $z_{j+1}$  before shifting. If  $\tau \leq T_{i+1}$ , then the leg  $z'_i, z_i$  does not intersect leg  $z'_{i+2}, z_{i+2}$ . The absolute value of the slope of the leg  $z'_i, z_i$  after convexifying  $z'_i$  is less than  $v/\tau$ . The slope of the leg is also between the slopes of  $z'_i, z'_{i-1}$  and  $z'_i, z'_{i+1}$ . The absolute value of these slopes is larger than  $(2-2v)/(S/2)$  which is the minimum possible slope of a segment of  $Z'$  in  $R$ . Define  $T = \min_j T_j$ . Hence, if  $v/T < (2-2v)/(S/2) = 4(1-v)/S$ , then  $\tau < T$ . We thus have an inequality that we want to be true for  $v$ :

$$v \leq \frac{4T}{S + 4T}. \quad (\text{B1})$$

Observe that convexifying  $z'_{i+1}$  may require a shift of  $z'_{i+1}$  by  $\delta'$  (and a compensating shift of  $z_{i+1}$  by  $\tau'$ ) after  $z'_i$  has been convexified. However, if  $v \leq 1/4$ , then balancing area and (B1) imply  $\frac{1}{4}T > v\tau' = \delta'(2-v) \geq \delta' \frac{7}{4}$  whence  $\delta' \leq T/7$ . This shows that  $z'_{i+1}$  stays on the right side of the old midpoint of  $z'_{i-1}$  and  $z'_{i+1}$  so that the corners at  $z'_i$  stay convex.

The next step of the construction is to place equidistant points on each of the legs. The segments between two consecutive points on the leg  $z'_i, z_i$  will serve as sides for quadrangles of the quadrangular subdivision of  $F_{i-1}$  and  $F_{i+1}$ . Specifically, a leg  $z'_i, z_i$  with  $i$  odd is subdivided into  $k-1$  segments of equal length and a leg  $z'_i, z_i$  with  $i$  even is subdivided into  $m-k$  segments. Recall that  $k$  is the number of rows in  $A^t$ . For the partition of  $F_i$  into 4-gons with the prescribed areas we proceed inductively as in Lemma 2. We again need a partition lemma, whose proof is in Appendix A.

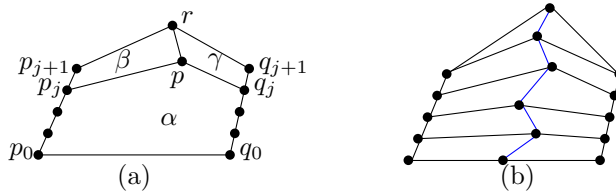


**Fig. 6.** (a) The  $\alpha$ ,  $\beta$  and  $\gamma$  partition of  $F$ . (b) A final partition of  $F_i$ .

**Lemma 4.** Consider a convex 5-gon  $F$  as shown in Fig. 6(a). Let  $\alpha$ ,  $\beta$ ,  $\gamma$  be positive numbers with  $\alpha + \beta + \gamma = \text{Area}(F)$ . If  $\alpha > \text{Area}(\square p_0, q_0, q_j, p_j)$ ,  $\beta > \text{Area}(\triangle p_j, r, p_{j+1})$ ,  $\gamma > \text{Area}(\triangle q_j, q_{j+1}, r)$ , then there exists  $p \in F$  such that  $\alpha = \text{Area}(\square p_0, q_0, q_j, p, p_j)$ ,  $\beta = \text{Area}(\square p_j, p, r, p_{j+1})$ ,  $\gamma = \text{Area}(\square q_j, q_{j+1}, r, p)$ .



To ensure that the conditions for Lemma 4 are satisfied throughout the inductive partition of the regions  $F_i$  we need to bound  $v$ . Let  $M = \min_{i,j} A_{i,j}$  be the minimum value in the table. Recall that  $S/2$  is the width of  $R$ , and the  $y$ -distance of  $p_j$  and  $p_{j+1}$  is at most  $v$ . Hence,  $vS/2$  is a generous upper bound on  $\text{Area}(\triangle p_j, r, p_{j+1})$ ,  $\text{Area}(\triangle q_j, q_{j+1}, r)$ , and  $\text{Area}(\square p_0, q_0, q_j, p_j)$ . We ensure that these areas are less than  $\beta$ ,  $\gamma$ , and  $\alpha$  respectively by requiring

$$v < \frac{2M}{S} \tag{B2}$$

**Theorem 2.** *Let  $A$  be a  $m \times n$  table of non-negative numbers  $A_{i,j}$ . Let  $R$  be a rectangle of width  $w$  and height  $h$  such that  $w \cdot h = \sum_{i,j} A_{i,j}$ . Then there exists a non-degenerate cartogram of  $A$  in  $R$  such that every face in the cartogram is convex. The construction requires  $O(mn)$  arithmetic operations.*

*Proof.* The steps of the construction are:

- Construct the table cartogram with degeneracies.
- Compute the bounds and fix an appropriate value for  $v$ , compute the skeleton  $G'$  and its regions  $F_i$ , and convexify the legs in order of increasing index.
- Subdivide each of the regions  $F_i$  into convex 4-gons (and two triangles).
- Remove the edges of the zig-zag to get the cells of the middle row as unions of two triangles.

All can be done with  $O(mn)$  arithmetic operations. Regarding the degeneracies, however, there is an issue that remains. To break  $A$  into  $A^t$  and  $A^b$ , we split row  $k$  so that the last row of  $A^t$  is a  $\lambda$ -fraction of row  $k$  from  $A$  while the rest of this row becomes the first row of  $A^b$ . Degeneracies occur if  $\lambda = 1$ . However, rather than splitting row  $k$  in this case, we can treat cells of row  $k$  as generic cells and assign a section of a leg to each of them. The construction is almost as before. Two details have to be changed. The first partition of each  $F_i$  into three pieces now produces two 4-gons and a 5-gon, before (see Fig. 6(b)) we had two triangles and a 5-gon in this step. The other change is that we don't remove zig-zag edges belonging to  $Z'$  to merge triangles to 4-gons at the end of the construction.  $\square$

Instead of just knowing that there are no degeneracies, it would be nice to have a lower bound on the *feature size*, that is the minimum side-length of a 4-gon in the table cartogram. The segments subdividing the legs have length at least  $v/m$ . Because these leg segments have length at most  $v$  and  $vS/2 < M$  (by (B2)), the opposite edges in a generic 4-gon (the blue edges in Fig. 6(b)) have length at least  $v$ . However, the triangles whose composition creates the 4-gons representing cells of row  $k$  can have area smaller than  $M$ . These triangles may have area  $\hat{\lambda}M$  where  $\hat{\lambda} = \min\{\lambda, 1 - \lambda\}$ . This may lead to a very small feature size. To improve on this, another degree of freedom in the construction can be used. Instead of breaking each cell  $A_{k,j}$  into a  $\lambda$  and a  $1 - \lambda$  fraction, we can use individual values  $\lambda_j$  to define  $A_{k,j}^t = \lambda_j A_{k,j}$ . The choice of the values  $\lambda_j$  must satisfy two conditions: (1)  $\sum_j \lambda_j A_{k,j} = \lambda S_k = \lambda \sum_j A_{k,j}$  and (2) if  $\lambda_i = 0$  and  $\lambda_j = 1$  then  $|i - j| > 1$ . By choosing most of the  $\lambda_j$  to be 0 or 1, and avoiding degeneracies as explained in the proof, we may be able to obtain a substantial improvement in feature size.

### 3 Generalizations

We can generalize many of our previous results in several ways. A more complete version of this section, including proofs, appears in Appendix B.

We generalize the notion of “area” by specifying the weight of a region as an integral over some density function  $w : R \rightarrow \mathbb{R}^+$ . The density function should be *positive*, meaning that the integrals over triangular regions with nonempty interiors exist and are positive. The following generalizes Lemma 1 for any positive density function, allowing us to compute cartograms on weighted  $\mathbb{R}^2$ .

**Lemma 5 (Weighted Triangle Lemma).** *Let  $\triangle abc$  be a triangle and  $w : \triangle abc \rightarrow \mathbb{R}^+$  be a positive density function on  $\triangle abc$ . Let  $\text{Area}(\triangle abc)$  be the  $w$ -weighted area of the triangle  $\triangle abc$ . Given three non-negative real numbers  $\alpha, \beta, \gamma$ , where  $\alpha + \beta + \gamma = \text{Area}(\triangle abc)$ , there exists a unique point  $p$  inside  $\triangle abc$  such that  $\text{Area}(\triangle pbc) = \alpha$ ,  $\text{Area}(\triangle apc) = \beta$ , and  $\text{Area}(\triangle abp) = \gamma$ .*

We now discuss some scenarios where the outface of the cartogram has a more general shape. The following theorem considers the case when the outface is a convex quadrangle  $\square pqrs$ . In such a case, we use a binary search to find the zigzag path that starts at  $q$  and ends at  $r$  or  $s$ .

**Theorem 3.** *Let  $A$  be a  $m \times n$  table of non-negative numbers. Let  $\square pqrs$  be an arbitrary convex quadrilateral with area equal to the sum,  $S$ , of the numbers of  $A$ . Then there exists a cartogram of  $A$  in  $\square pqrs$  (with degeneracies).*

Next, we show how to compute a table cartogram inside a circle. A *circular triangle*  $\triangle abc$  is a region in the plane bounded by three circular arcs (called *arms*) that pairwise meet at the points  $a, b$ , and  $c$  (called *vertices*), such that for every vertex  $v \in \{a, b, c\}$  and for every point  $x$  on the arc that is not incident to  $v$ , one can draw a circular arc between  $v$  and  $x$  inside  $\triangle abc$  that does not cross the boundary of  $\triangle abc$ . An arm is *convex* if the straight line joining any two points on the arm is interior to the region bounded by the triangle. Otherwise, the arm is *concave*. We distinguish four types of circular triangles, see Figs. 7(a–d). We generalize Lemma 1 for circular triangles, i.e., given a circular triangle, one can split it into three other circular triangles with prescribed areas, and find the following generalization of Theorem 1.

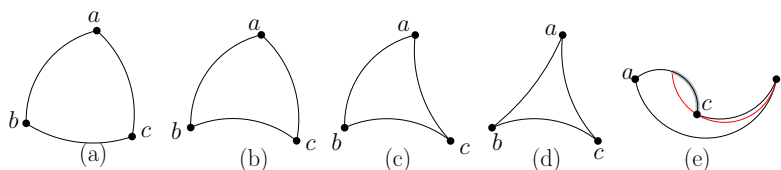


**Fig. 7.** (a–d) A circular triangle of Type  $i$ ,  $1 \leq i \leq 4$ , i.e., a circular triangle with  $i$  concave arms. (e) A region bounded by circular arcs, but not a circular triangle.

**Theorem 4.** *Let  $A$  be a  $m \times n$  table of non-negative numbers. Let  $C$  be an arbitrary circle with area equal to the sum of the numbers of  $A$ . Then there exists a cartogram of  $A$  in  $C$  where every face is a circular triangle.*

We now show that one can compute a cartogram of a table on the surface of a sphere. There are several well studied area preserving map projection techniques. Here we use Lambert’s cylindrical equal-area projection. The construction used is shown in Fig. 8.

**Theorem 5.** *Every  $m \times n$  table of non-negative numbers admits a cartogram on a sphere.*

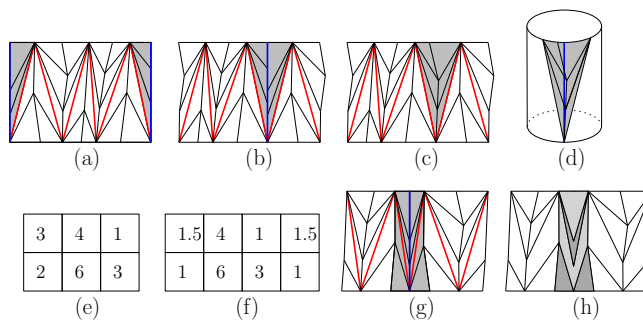


**Fig. 8.** Cylindrical cartogram construction. (a–d)  $n$  is even, (e–h)  $n$  is odd. Note that when  $n$  is even, the faces are convex quadrilaterals. However, when  $n$  is odd, the faces with areas from the leftmost column of  $A$  may be concave hexagons.

## 4 Conclusions and Future Work

We have presented a simple constructive algorithm that realizes any table inside a rectangle in which each cell is represented by a convex quadrilateral with its prescribed weight. If all weights are strictly positive, then we can also obtain non-degenerate realizations. This method can be further extended to realize any table inside an arbitrary convex quadrilateral, inside a circle using circular arcs, or even on a sphere. From a practical point of view, the cartograms obtained by our method may not be visually pleasing, but by using additional straightforward heuristics that improve the visual quality while keeping the areas the same, we can obtain cartograms of practical relevance, as shown in Figs. 1 and 3. Our theoretical solution plays a vital role in this context, since heuristics used directly may get stuck, being unable to obtain the correct areas. Whether there exists a method that can gradually change the areas to provably obtain the correct areas remains an interesting open problem. It would also be interesting to examine table cartograms for other types of tables, such as triangular or hexagonal grids. From a theoretical point of view, finding algorithms for table cartograms on a sphere with less distortion, and generalizing our result to 3D table cartograms (inside a box) are further interesting open problems.

**Acknowledgments.** Initial work on this problem began at Dagstuhl Seminar 12261 “Putting Data on the Map” in June 2012 and most of the results of this paper were obtained at the Barbados Computational Geometry workshop in February 2013. We would like to thank the organizers of these events, as well as many participants for fruitful discussions and suggestions.

## References

1. M. J. Alam, T. Biedl, S. Felsner, M. Kaufmann, and S. G. Kobourov. Proportional contact representations of planar graphs. *Journal of Graph Algorithms and Applications*, 16(3):701–728, 2012.
2. M. J. Alam, T. Biedl, S. Felsner, M. Kaufmann, S. G. Kobourov, and T. Ueckerdt. Computing cartograms with optimal complexity. In *SoCG’12*, pages 21–30, 2012.
3. H. S. M. Coxeter. *Introduction to Geometry*. Wiley, New York, 2nd edition, 1969.
4. M. de Berg, E. Mumford, and B. Speckmann. On rectilinear duals for vertex-weighted plane graphs. *Discrete Mathematics*, 309(7):1794–1812, 2009.
5. D. Dorling. *Area cartograms: their use and creation*. Number 59 in Concepts and Techniques in Modern Geography. University of East Anglia, 1996.
6. J. A. Dougenik, N. R. Chrisman, and D. R. Niemeyer. An algorithm to construct continuous area cartograms. *The Professional Geographer*, 37(1):75–81, 1985.
7. H. Edelsbrunner and R. Waupotitsch. A combinatorial approach to cartograms. *Computational Geometry: Theory and Applications*, 7(5–6):343–360, 1997.
8. D. Eppstein, E. Mumford, B. Speckmann, and K. Verbeek. Area-universal rectangular layouts. In *SoCG’09*, pages 267–276. ACM, 2009.
9. D. Eppstein, M. van Kreveld, B. Speckmann, and F. Staals. Improved grid map layout by point set matching. In *Proc. of PacificVis’13*, page To appear., 2013.
10. T. G. Feeman. *Portraits of the Earth: A Mathematician Looks at Maps*. American Mathematical Society, September 30 2002.
11. M. T. Gastner and M. E. J. Newman. Diffusion-based method for producing density-equalizing maps. *National Academy of Sciences*, 101(20):7499–7504, 2004.
12. R. Heilmann, D. A. Keim, C. Panse, and M. Sips. Recmap: Rectangular map approximations. In *Proc. of InfoVis’04*, pages 33–40, 2004.
13. D. H. House and C. J. Kocmoud. Continuous cartogram construction. In *Proc. of VIS’98*, pages 197–204, 1998.
14. D. A. Keim, S. C. North, and C. Panse. Cartodraw: A fast algorithm for generating contiguous cartograms. *IEEE Trans. Vis. Comput. Graph.*, 10(1):95–110, 2004.
15. B. Knaster, C. Kuratowski, and S. Mazurkiewicz. Ein beweis des fixpunktsatzes für  $n$ -dimensionale simplexe. *Fundamenta Mathematicae*, 14:132–137, 1929.
16. E. Raisz. The rectangular statistical cartogram. *Geographical Review*, 24(2):292–296, 1934.
17. J. P. Snyder. *Map Projections—A Working Manual*. U. S. Geological Survey Professional Paper 1935, Washington, DC: U. S. Government Printing Office, 1987.
18. W. Tobler. Thirty five years of computer cartograms. *Annals Assoc. American Geographers*, 94(1):58–73, 2004.
19. M. van Kreveld and B. Speckmann. On rectangular cartograms. *Comput. Geom. Theory Appl.*, 37(3):175–187, 2007.
20. J. Wood and J. Dykes. Spatially ordered treemaps. *IEEE Transactions on Visualization and Computer Graphics*, 14(6):1348–1355, 2008.
21. K.-H. Yeap and M. Sarrafzadeh. Floor-planning by graph dualization: 2-concave rectilinear modules. *SIAM J. Comput.*, 22(3):500–526, 1993.

## A Proofs

In this section we include additional details that are omitted in the main text due to space constraints.

The following lemma is a consequence of properties of barycentric coordinates, but we include a proof for completeness.

**Lemma 1 (Triangle Lemma).** *Let  $\triangle abc$  be a triangle and let  $\alpha, \beta, \gamma$  be non-negative numbers, where  $\alpha + \beta + \gamma = \text{Area}(\triangle abc)$ . Then we can find a point  $p$  in  $\triangle abc$ , where  $\text{Area}(\triangle pbc) = \alpha$ ,  $\text{Area}(\triangle apc) = \beta$ ,  $\text{Area}(\triangle abp) = \gamma$ , in  $O(1)$  arithmetic operations.*

*Proof.* Let  $\ell_a$  be the line such that a triangle with side  $bc$  and a corner on  $\ell_a$  has area  $\alpha$ . This line intersects segments  $ab$  and  $ac$ . Let  $\ell_b$  be the line such that a triangle with side  $ac$  and a corner on  $\ell_b$  has area  $\beta$ . This line intersects segments  $ab$  and  $bc$ . Let  $q_a$  be the intersection point of line  $\ell_a$  with segment  $ab$  and let  $q_b$  be the the intersection point with line  $\ell_b$ . Assume that the order of points on segment  $ab$  is  $a, q_a, q_b, b$ , then the triangles  $\triangle q_a bc$  and  $\triangle a q_b c$  cover the triangle  $\triangle abc$  so that  $\text{Area}(\triangle abc) < \alpha + \beta$ . This contradiction shows that the order of points on segment  $ab$  is  $a, q_b, q_a, b$ . Hence  $\ell_a$  and  $\ell_b$  intersect in a point  $p$  inside of  $\triangle abc$ . This point  $p$  has the desired properties.

Note that  $p$  can be computed with  $O(1)$  arithmetic operations. □

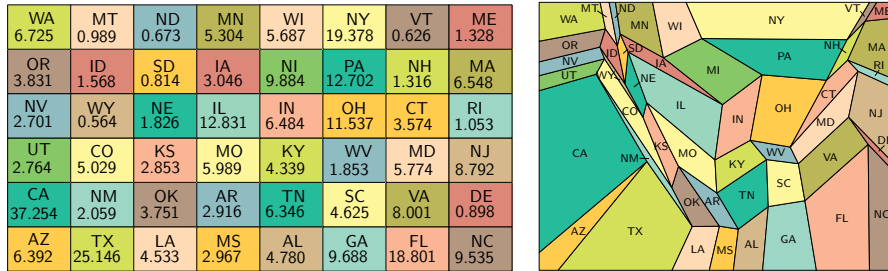


**Fig. 9.** The population data table for USA in millions in 2010 and a table cartogram of USA according to the population of the states in 2010, using the grid map of [9].

**Lemma 4** *Consider a convex 5-gon  $F$  as shown in Fig. 6(a). If  $\alpha, \beta$  and  $\gamma$  are positive numbers with  $\alpha + \beta + \gamma = \text{Area}(F)$ . If  $\alpha > \text{Area}(\square p_0, q_0, q_j, p_j)$  and  $\beta > \text{Area}(\triangle p_j, r, p_{j+1})$  and  $\gamma > \text{Area}(\triangle q_j, q_{j+1}, r)$ , then there is a point  $p \in F$  such that  $\alpha = \text{Area}(\square p_0, q_0, q_j, p, p_j)$  and  $\beta = \text{Area}(\square p_j, p, r, p_{j+1})$  and  $\gamma = \text{Area}(\square q_j, q_{j+1}, r, p)$ .*

*Proof.* The assumptions imply that if  $p$  exists it has to be in the interior of the triangle  $\triangle p_j, r, q_j$ . The existence follows from Lemma 1. □

## B Generalizations

One direction for generalizations is to generalize the notion of “area”. This can be done by specifying the weight of a region as an integral over some density function  $w : R \rightarrow \mathbb{R}^+$ . The density function should have the property that the integrals over triangular regions with nonempty interiors exist and are positive. We call such a density function positive.

The following lemma can be proved (even for higher dimensions) using the Knaster-Kuratowski-Mazurkiewicz lemma [15]. It can also be deduced in the context of barycentric coordinate systems [3].

**Lemma 5 (Weighted Triangle Lemma).** *Let  $\triangle abc$  be a triangle and  $w : \triangle abc \rightarrow \mathbb{R}^+$  be a positive density function on  $\triangle abc$ . Let  $\text{Area}(\triangle abc)$  be the  $w$ -weighted area of the triangle  $\triangle abc$ . Given three non-negative real numbers  $\alpha, \beta, \gamma$ , where  $\alpha + \beta + \gamma = \text{Area}(\triangle abc)$ , there exists a unique point  $p$  inside  $\triangle abc$  such that  $\text{Area}(\triangle pbc) = \alpha$ ,  $\text{Area}(\triangle apc) = \beta$ , and  $\text{Area}(\triangle abp) = \gamma$ .*

*Proof.* Let  $\rho$  be a ray starting at  $a$  and intersecting the segment  $bc$ . Since  $w$  is a positive density function,  $\text{Area}_w(\triangle xbc)$  is strictly decreasing as  $x$  moves from  $a$  along  $\rho$ . Hence there is a unique point  $x(\rho)$  on  $\rho$  such that  $\text{Area}_w(\triangle x(\rho)bc) = \alpha$ . The points  $x(\rho)$  for all different  $\rho$  trace a simple curve  $C_a$  in  $\triangle abc$  that separates  $a$  from  $bc$ . This curve has a point on  $ab$  and a point on  $ac$ . Similarly, we get a curve  $C_b$  that intersects every ray from  $b$  to  $ac$  at a point  $x$  with  $\text{Area}_w(\triangle axc) = \beta$ .

Let  $q_a$  and  $q_b$  be the intersection points of  $C_a$  and  $C_b$  with segment  $ab$ . Assume that the order of points on segment  $ab$  is  $a, q_a, q_b, b$ , then the triangles  $\triangle q_a bc$  and  $\triangle a q_b c$  cover the triangle  $\triangle abc$  so that  $\text{Area}_w(\triangle abc) < \alpha + \beta$ . This contradiction shows that the order of points on segment  $ab$  is  $a, q_b, q_a, b$ . Hence  $C_a$  and  $C_b$  intersect at a point  $p$  inside of  $\triangle abc$ . This point  $p$  has the desired properties.

Assume that  $p$  and  $p'$  are two points with the desired properties. Then there is a pair  $y, z$  among  $a, b, c$  such that  $\triangle(pyz) \subset \triangle(p'yz)$  and hence  $\text{Area}_w(\triangle pyz) < \text{Area}_w(\triangle p'yz)$ . This contradiction proves uniqueness.  $\square$

### B.1 Cartogram in an arbitrary convex quadrilateral

We show that every table can be represented as a cartogram in any arbitrary convex quadrilateral with area equal to the sum of the numbers in the table.

**Theorem 3.** *Let  $A$  be a table with  $m$  rows and  $n$  columns of non-negative numbers. Let  $\square pqrs$  be an arbitrary convex quadrilateral with area equal to the sum,  $S$ , of the numbers of  $A$ . Then there exists a cartogram of  $A$  in  $\square pqrs$  (with degeneracies).*

*Proof.* If  $\square pqrs$  is a convex quadrilateral that is not a rectangle, we use binary search to find the zigzag path that starts at  $q$  and ends at  $r$  or  $s$  and realizes the required areas for the intermediate triangles. By continuity, such a zigzag path always exists. Note that such a zigzag path does not necessarily split  $A$

into two equal halves, rather, the row  $k$  of  $A$  that determines  $A^t$  and  $A^b$  satisfies  $\sum_{1 \leq i \leq k-1} S_i + \lambda S_k = \alpha S$  for some  $\alpha \in (0, 1]$ , which we determine by binary search. Figs. 10(a-c) illustrates such a binary search.

When  $\alpha$  is found, we can continue as in the proof of Theorem 1. □

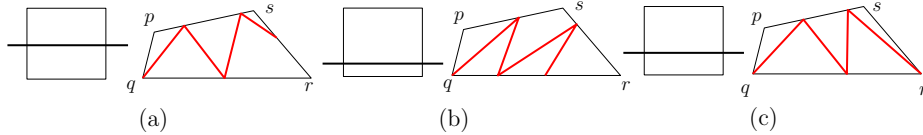


**Fig. 10.** Finding a division of  $A$  such that  $Z$  starts at  $q$  and ends at  $r$ . (a-c) Some steps of the binary search. (a) For some split of the table,  $Z$  ends before reaching  $r$ , and hence we need to update the split. (b)  $Z$  ends after  $r$ . (c) The final step of the search, where the endpoint of  $Z$  hits  $r$ .

## B.2 Table Cartograms in a Circle

In this section we show that any table  $A$  of size  $m \times n$  of non-negative weights admits a cartogram inside a circle with area equal to the sum of the numbers of  $A$ , and every edge in the cartogram is represented as a circular arc. To prove the existence of such a cartogram, we modify the proof of Lemma 5.

A *circular triangle*  $\triangle abc$  is a region in the plane bounded by three circular arcs (called *arms*) that pairwise meet at the points  $a$ ,  $b$ , and  $c$  (called *vertices*), such that for every vertex  $v \in \{a, b, c\}$  and for every point  $x$  on the arc that is not incident to  $v$ , one can draw a circular arc between  $v$  and  $x$  inside  $\triangle abc$  that does not cross the boundary of  $\triangle abc$ . Figs. 7(a-d) are circular triangles, but Fig. 7(e) is not a circular triangle since no circular arc connects vertex  $b$  to the shaded part of arc  $ac$ . By definition, a circle is a circular triangle, where all three arms are the arcs of a single circle. An arm of a circular triangle is *convex* if the straight line joining any two points on the arm is interior to the region bounded by the triangle. Otherwise, the arm is *concave*. Depending on the number of convex arms, we distinguish four types of circular triangles. Figs. 7(a-d) shows these four types of circular triangles.

**Lemma 6 (Arc-Triangle Lemma).** *Let  $\triangle abc$  be an arbitrary circular triangle of Type  $i$ , where  $i \in \{0, 1, 2, 3\}$ . Given three non-negative real numbers  $\alpha$ ,  $\beta$ ,  $\gamma$ , where  $\alpha + \beta + \gamma = \text{Area}(\triangle abc)$ , there exists a point  $p$  inside  $\triangle abc$  such that  $\text{Area}(\triangle pbc) = \alpha$ ,  $\text{Area}(\triangle apc) = \beta$ , and  $\text{Area}(\triangle abp) = \gamma$ , and every circular triangle among  $\triangle pbc$ ,  $\triangle apc$  and  $\triangle abp$  is of Type  $i$  for some  $i \in \{0, 1, 2, 3\}$ .*

*Proof.* For every vertex  $v \in \triangle abc$ , we first define a set  $S_v$  of *geodesic rays* that start at  $v$ , end at the arm that does not contain  $v$ , and satisfy the following properties.

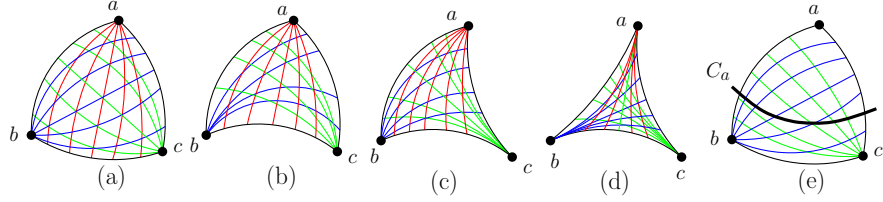


**Fig. 11.** (a–d) A circular triangle with no concave arm (Type 0), one concave arm (Type 1), two concave arms (Type 2), and three concave arms (Type 3). (e) A region bounded by circular arcs, but not a circular triangle. (f–i) The sets of geodesic rays. (j) Illustrating  $C_x$ .

- (a) Each ray of  $S_v$  is a circular arc that splits  $\triangle abc$  into two circular triangles that we call the left or right circular triangle depending on the side of ray the triangle lies in.
- (b) For each point  $x$  in  $\triangle abc$ , there exists a ray in  $S_v$  that passes through  $x$ .
- (c) Consider the rays in  $S_v$  in clockwise order. Then the area of the left circular triangle increases continuously and monotonically from 0 to  $Area(\triangle abc)$ .

Figs. 11(a–d) illustrate  $S_a, S_b$  and  $S_c$  for different types of circular triangles. The proof is now similar to the proof of Lemma 5. We first find the trace  $C_a$  of a point  $x$  inside  $\triangle abc$  such that  $Area(\triangle xbc) = \alpha$ , as shown in Fig. 11(e). Note that the arms  $bx$  and  $cx$  of  $\triangle xbc$  are determined by the rays of  $S_b$  and  $S_c$  that pass through  $x$ . Therefore, each ray in  $S_a$  can be intersected by  $C_a$  at most once. We define  $C_b$  with respect to  $S_b$  analogously. In a similar way to the proof of Lemma 5, we can prove that  $C_a$  and  $C_b$  intersect at a single point  $p$  such that  $Area(\triangle pbc) = \alpha$ ,  $Area(\triangle apc) = \beta$ , and  $Area(\triangle abp) = \gamma$ . It is straightforward to verify that each of  $\triangle pbc$ ,  $\triangle apc$ , and  $\triangle abp$  must be a circular triangle of Type  $i$ , for some  $i \in \{0, 1, 2, 3\}$ .  $\square$

Let  $G$  be an arbitrary plane 3-tree such the internal faces of  $G$  are assigned non-negative weights. Given a circular triangle  $\triangle abc$  of Type  $i$ , where  $i \in \{0, 1, 2, 3\}$  such that  $Area(\triangle abc)$  is equal to the sum of the face weights of  $G$ , one can use Lemma 6 to obtain a drawing of  $G$  inside  $\triangle abc$  where the faces are drawn as circular triangles respecting the prescribed face weights.

**Lemma 7.** *Let  $G$  be an arbitrary plane 3-tree such the internal faces of  $G$  are assigned non-negative weights. Let  $\triangle abc$  be a circular triangle of Type  $i$ , where  $i \in \{0, 1, 2, 3\}$  and  $Area(\triangle abc)$  is equal to the sum of the face weights of  $G$ . Then there exists a drawing of  $G$  inside  $\triangle abc$  such that each face of  $G$  is drawn as a circular triangle of type 0, 1, 2 or 3 with area equal to its prescribed weight.*

We are now ready prove the main result of this section.

**Theorem 6.** *Let  $A$  be a table with  $m$  rows and  $n$  columns of non-negative numbers. Let  $C$  be an arbitrary circle with area equal to the sum of the numbers of  $A$ . Then there exists a cartogram of  $A$  in  $C$  where every face is a circular triangle. If all numbers in  $A$  are positive then the cartogram is perfect.*



*Proof.* Similar to the proof of Theorem 3, we first find the largest index  $k$  such that the sum of the numbers in rows  $1, 2, \dots, k-1$  is less than  $S/2$ . We may choose  $\lambda \in (0, 1]$  such that  $\sum_{1 \leq i \leq k-1} S_i + \lambda S_k = S/2$ . We then define the tables  $A^t$  and  $A^b$  with respect to row  $k$ . We next find a zigzag path in  $G$  that divides the circle into circular triangles of Type 0. Finally, we use Lemma 6 to compute the cartograms of the columns of  $A^t$  and  $A^b$  that correspond to those circular triangles, and remove the segments on the zigzag path to merge the cells corresponding to the row  $k$  of  $A$ .  $\square$

### B.3 Table Cartogram on a Sphere

In this section we show that one can compute a cartogram of a table on the surface of a sphere. The idea is to first construct a cartogram<sup>1</sup> of the table on a cylinder, and then use the map projection techniques that preserve area [10, 17] to find a cartogram on the sphere. There are several well studied area preserving map projection techniques such as Lambert’s cylindrical equal-area projection, Lambert azimuthal equal-area projection, or Hammer-Aitoff Equal-Area Projection. Here we use Lambert’s cylindrical equal-area projection.

**Lemma 8.** *Let  $A$  be a  $m \times n$  table of non-negative numbers. Let  $H$  be a cylinder with surface area equal to the sum of the numbers of  $A$ . Then there exists a cartogram of  $A$  on  $H$ .*

*Proof.* The case when  $n = 1$  is straightforward. Therefore, we assume that  $n \geq 2$ . Let  $h$  be the height and  $r$  be the radius of  $H$ . If  $n$  is even, then we first compute a cartogram on a rectangle  $H$  of height  $h$  and width  $2\pi r$  in a similar way as in the proof of Theorem 3. However, the vertices on the left side of  $H$  may not match the vertices on the right side of  $H$  when we wrap  $H$  into a cylinder. So we merge the leftmost and rightmost triangles formed by the zigzag path in  $H$  and find the cartogram of columns 1 and  $n$  of  $A^t$  in the resulting triangle using Lemma 2. This process is shown in Figs. 8(a–d).

If  $n$  is odd, we equally divide the leftmost column into two columns and move one of these columns to the right of  $A$ , as shown in Figs. 8(e–f). We then compute the cartogram, as in the case when  $n$  is even, and remove the segments that separate the divided leftmost column of  $A^t$ , and the (infinitesimal) segments that separate the divided leftmost column of  $A^b$ , as in Fig. 8(g–h).

In both of these cases, we can compute a perfect cartogram if all numbers in  $A$  are positive, as in Theorem 3. When  $n$  is even, the faces are convex quadrilaterals. However, when  $n$  is odd, the faces with areas from the leftmost column of  $A$  may be concave hexagons, as shown in Fig. 8(h).  $\square$

We now use Lambert’s cylindrical equal-area projection to find a cartogram of  $A$  on the sphere.

**Theorem 7.** *Every  $m \times n$  table of non-negative numbers admits a cartogram on a sphere.*

<sup>1</sup> This cartogram may have non-convex faces.

A major problem of using an equal area projection to compute cartograms on a sphere is the distortion of shapes. Therefore, it is worth investigating new algorithms that can produce aesthetically pleasing cartograms on a sphere.